2012

Development of an In-Cylinder Heat Transfer Correlation for Reciprocating Compressors

Fernanda P. Disconzi
deschamps@polo.ufsc.br

Cesar J. Deschamps

Evandro L. L. Pereira

Development of an In-Cylinder Heat Transfer Correlation for Reciprocating Compressors

Fernanda P. DISCONZI[1], Evandro L.L. PEREIRA[2], Cesar J. DESCHAMPS[1]*

[1]POLO Research Laboratories for Emerging Technologies in Cooling and Thermophysics
Federal University of Santa Catarina
Florianopolis, SC, Brazil
deschamps@polo.ufsc.br

[2]Embraco
Rua Rui Barbosa, 1020
89219-901, Joinville, SC, Brazil
Evandro_L_Lange@embraco.com.br

* Corresponding Author

ABSTRACT

The gas superheating that takes place throughout the suction system and inside the cylinder of reciprocating compressors adversely affects their overall efficiency. Simulation models adopted in the design of reciprocating compressors are generally based on lumped formulation and rely on empirical correlations for different physical phenomena, including the gas-to-wall heat transfer in the cylinder. The present paper reports a numerical study of heat transfer inside the cylinder of a simplified geometry of reciprocating compressor, considering the effect of fluid flow through the valves. Predictions for the instantaneous heat transfer at the walls are obtained for actual operating conditions and compared with estimates given by correlations commonly adopted for reciprocating compressors. It is shown that the increase of heat transfer during the suction and discharge processes is not properly accounted for by such correlations. Based on the predictions, a new correlation for the in-cylinder heat transfer is put forward and tested in different operating conditions.

1. INTRODUCTION

Most studies in the literature on heat transfer inside cylinders are focused on internal combustion engines, both experimentally (Overbye et al., 1961; Annand, 1963; Woschni, 1967; Rakopoulos and Mavropoulos, 2000) and numerically (Mohammadi et al., 2008, Mohammadi and Yaghoubi, 2010; Rakopoulos et al., 2010). Very early it was found that the gas thermal capacity may give rise to a phase lag between the bulk gas-wall temperature difference and the resulting flux at the surface (Overbye et al., 1961) during compression and expansion processes. The Nusselt number correlations derived in such studies are quite different. For instance, Annand (1963) expressed the Nusselt number as a function of a Reynolds number based on the piston mean velocity, whereas Woschni (1967) assumed a correlation based on the average velocity of the gas and instantaneous values of pressure and temperature in the cylinder.

Arguably, the first attempt to experimentally investigate heat transfer in the cylinder of reciprocating compressors was made by Adair *et al*. (1972). The authors proposed a correlation for Nusselt number, $Nu = 0.053\, Re^{0.8} Pr^{0.6}$, in which the Reynolds number was expressed in terms of a velocity proportional to the crankshaft speed. Later, Brok *et al*. (1980) carried out simulations of a reciprocating compressor accounting for internal heat transfer, introducing modifications into the correlation proposed by Adair *et al*. (1972). Liu and Zhou (1984) measured the temperature distribution at the cylinder wall for different pressure ratios, suction temperatures and compressor speed, and derived a heat transfer correlation by applying the first law of thermodynamics. By using the same velocity characteristic adopted by Adair *et al*. (1972), the authors derived a similar expression for the Nusselt number but with a quite

different constant of proportionality: $Nu = 0.75\, Re^{0.8} Pr^{0.6}$. Hsieh and Wu (1996) proposed a correlation without reference to the Prandtl number, but incorporating the variation of viscosity to emphasize pressure effect on gas property. In order to account for the increase of gas velocity during discharge process, an additional term, $C_1\, Re_1$, was added into the final correlation: $Nu = (C_1\, Re_1 + C_2 Re^{C_3})(\mu/\mu_0)^{C_4}$, where μ_0 (= 1.76×10^{-5} Pa.s) is the viscosity of nitrogen at 1 atm and 20°C. Different values for C_1, C_2, C_3 and C_4 were adopted for each thermodynamic process of the compression cycle.

Fagotti *et al*. (1994) made an assessment of different heat transfer correlations with reference to experimental data of temperature for a small hermetic reciprocating compressor. According to the authors, the correlation of Liu and Zhou (1984) gives rise to inconsistent results for some working conditions. Better agreements were verified with the correlations of Brok et al. (1980), Adair et al. (1972) and Annand (1963), with the latter being the proposal that best fitted the experimental data.

This paper reports a numerical analysis of the in-cylinder heat transfer process in a small reciprocating compressor adopted for household refrigeration. The simulation model is based on a two-dimensional formulation of the in-cylinder compressible turbulent flow and takes into account the effect of the suction and discharge processes. Numerical results for the instantaneous heat transfer at the walls are obtained for actual operating conditions and compared with estimates from correlations available in the literature. A new correlation for heat transfer in the cylinder of small reciprocating compressors is proposed and tested at different operating conditions.

2. MATHEMATICAL MODEL

The governing equations (mass, momentum and energy) of the compressible, turbulent flow is solved for averaged quantities in which a computed variable represents an ensemble value over many engine cycles at a specified spatial location. The RNG *k*-*ε* model was employed to estimate the turbulent transport following the eddy viscosity concept, μ_t. This version of *k*-*ε* model has an additional term in the equation for the turbulence dissipation *ε* that significantly improves its accuracy for rapidly strained flows, as verified in the flow through compressor valves (Salinas-Casanova et al., 1999). In addition to that, the RNG *k*-*ε* model provides an analytical relationship for the turbulent Prandtl number and an expression for the effective viscosity suitable for low-Reynolds-number condition.

Pereira *et al.* (2010) numerically investigated the turbulent heat transfer process inside the cylinder of a small reciprocating compressor including the flow through valves. Predictions of heat transfer revealed a significant influence of the flow through valves on the in-cylinder heat transfer, which is not properly described by available correlations. Rakopoulos *et al*. (2010) made an assessment of four wall functions widely used to predict heat transfer in reciprocating engines. Simulations were carried out with the standard *k*-*ε* model and comparisons between numerical and experimental results showed that all wall functions fail to adequately describe the instantaneous heat flux at the cylinder wall. Rakopoulos *et al*. (2010) have also shown that the standard wall function under-predicts heat transfer in the cylinder of reciprocating engines. In fact, Disconzi *et al.* (2011) have shown that the standard wall-function (Launder and Spalding, 1974) returns smaller levels of heat transfer at the cylinder walls of reciprocating compressor in comparison with predictions of near wall modeling approaches, especially in the late stage of the compression process and during the discharge process. The standard wall function has been a common choice for industrial applications but some authors argue that near wall modelling allows a more realistic description of convective heat transfer (Launder, 1984).

Considering the aforementioned aspects, a near wall modelling represented by the enhanced wall treatment (Kader, 1979) was chosen for the present study. The enhanced wall treatment is a near-wall modeling method combined with a two-layer model and it requires refined meshes ($y^+ \cong 1$) for the cells adjacent to the wall. In this approach, the cells are split into a viscous region and a fully turbulent region with reference to the turbulent Reynolds number $Re_y (= \rho y k^{1/2}/\mu)$. Following this two-layer approach, the RNG k-ε turbulence model is employed in the fully turbulent region ($Re_y > Re_y^*$; $\mathrm{Re}_y^* = 200$). In the near wall region ($Re_y < Re_y^*$) the one-equation model of Wolfstein (1969) is adopted instead.

3. SIMULATION PROCEDURE

Simulations were carried out for a 3000 rpm reciprocating compressor operating with R-134a under the ASHRAE LBP condition, characterized by the following evaporating and condensing conditions: (T_e = -23.3ºC; p_e = 115 kPa) and (T_c = 54.4ºC, p_c =1470 kPa). The geometric dimensions adopted for the model are representative of small reciprocating compressors commonly applied in domestic refrigeration: diameter of the cylinder bore D = 20 mm; piston stroke L = 20 mm; suction orifice diameter d_s = 7 mm; suction valve diameter D_s = 9 mm; discharge orifice diameter d_d = 6 mm; discharge valve diameter D_d = 8 mm.

The computational model was developed with a commercial code based on the finite volume method (ANSYS, 2010). Due to the presence of moving surfaces such as the piston and the suction and discharge valves, a moving grid strategy was applied to simulate the compression cycle. A simplified axisymmetric geometry was chosen for the analysis and, therefore, valves were centrally positioned in the compression chamber. The reed was considered to be parallel to the valve seat and its dynamics was represented by a single-degree-of-freedom model. For convenience, the suction and discharge processes were independently simulated. The discharge model simulates the compression and discharge processes, while the suction model includes the expansion and suction processes. Schematics of the solution domains and computational grids adopted to simulate both processes are depicted in Figures 1 and 2, respectively.

For the discharge model the simulation starts with the piston at the bottom dead center ($\omega t = 0^o$). The initial pressure and temperature of the gas inside the cylinder are estimated according to the compressor operating condition. On the other hand, when the suction model is considered, the simulation starts with the piston at the top dead center ($\omega t = 180^o$) and the initial temperature and pressure values inside the cylinder are taken from results previously obtained for the discharge process.

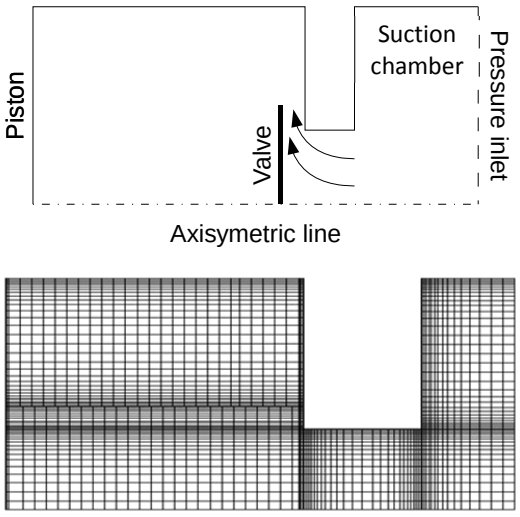

Figure 1: Solution domain and mesh for the suction model.

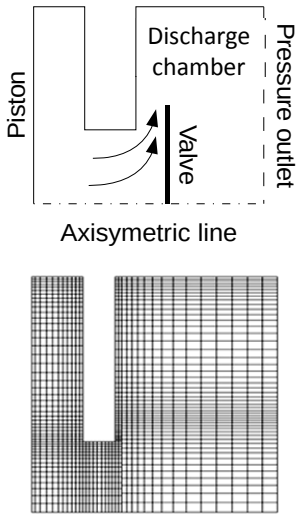

Figure 2: Solution domain and mesh for the discharge model.

Boundary conditions at inlet, walls, axis of symmetry and outlet are required. At the inlet boundary of the suction chamber, pressure and temperature were prescribed as p_s = 115 kPa and T_s = 57ºC. At the outlet boundary of the discharge chamber a condition of locally parabolic flow was assumed, but in the case of backflow the corresponding values for pressure and temperature were defined as p_d = 1470 kPa and T_d = 152ºC. Estimates for temperature at the boundaries of both chambers were made possible from experimental data. However, no information is available for the turbulence kinetic energy in such locations and a value of 6% of turbulence intensity was used in the calculation of all results shown in this study. Moreover, the dissipation rate was estimated based on the assumption of equilibrium boundary layer ($\varepsilon = C_\mu^{3/4} k^{3/2}/L_D$), where $L_D = 0.07\, D_H$, $C_\mu = 0.09$ and D_H = 0.02m.

All velocity components at the walls were set to zero, except for the reed and piston surfaces whose velocities were obtained from the reed valve dynamics and from the crankshaft mechanism, respectively. For the turbulence quantities k and ε rather than prescribing a condition at the walls, the enhanced wall treatment described in the previous section was adopted. The experimentally verified temperature of 87°C at the cylinder wall was specified as the boundary condition for the energy equation and kept constant throughout the simulation. Since the main focus of this study is the in-cylinder heat transfer, an adiabatic condition was assumed for all the remaining walls, such as the walls of valve orifices, suction chamber and discharge chamber. Finally, the normal velocity and the normal gradients of all other quantities were set to zero in the axis of symmetry.

A second-order upwind scheme was adopted to interpolate the flow quantities required at the faces of each cell of the computational grid. Analyses for grid and time discretizations were performed to verify truncation errors and guarantee the solution accuracy. Table 1 shows the results for net heat transfer in the cylinder emerging from the assessment of truncation errors in tests with three different levels of grid refinement (11×10^3, 22×10^3 and 44×10^3 control volumes). For the enhanced wall treatment the grid refinement was developed to ensure $y^+ \cong 1$ for the cell adjacent to the wall so as to properly resolve the viscous sub-layer. It is clear from Table 1 that the results for the two most refined grids are very close to each other. Hence, in order to reduce computing cost the second most refined grid (22×10^3) was used in the remaining calculations.

Table 1: Predictions of net heat transfer in the cylinder obtained with different grid refinements.

Number of Control Volumes	11×10^3	22×10^3	44×10^3
$\dot{Q}$ [W]	3,7	4,1	4,2

4. RESULTS

Heat flux predicted in the cylinder, Q, is shown in Figure 3 as a function of the crank angle, ωt. In order to assist the explanation of the main phenomena affecting heat transfer, the periods corresponding to each process of the compression cycle are identified in Figure 3: compression (A), discharge (B), expansion (C) and suction (D). Accordingly, the discharge (B) and suction (D) processes are approximately situated in the intervals 150°-190° and 216°-360°, respectively, as identified by the vertical dashed lines. Negative values in Figure 3 represent that heat is transferred from the gas to the cylinder wall, and vice-versa.

As can be seen, heat flux during the discharge process is much higher than that in the suction process. This occurs because the piston is very close to the cylinder head and, as a consequence, high levels of velocity are present in the flow along the small clearance left between the piston and the cylinder head as the gas is directed towards the discharge valve. It is also interesting to note the significant increase of heat transfer as the piston approaches the top dead center (I) due to the high temperature level the gas attains during compression. After the discharge valve opens, there is a peak of heat flux associated with gas compression and increase of flow velocity along the cylinder clearance (II). Finally, a second peak of heat flux occurs near the closing stage of the discharge valve (III), which was identified as a result of backflow in the valve.

Results for heat transfer rate in each of the surfaces that form the compression chamber are shown in Figure 4, together with the instantaneous mass flow rates in the suction and discharge valves. It is quite clear that the flow through the valves increases the heat flux in all surfaces. As the piston approaches the valve plate during compression, the fluid flow velocity along cylinder lateral surface is small and this is the reason for its reduced contribution on the total heat flux during the discharge process. It should be noticed that the piston is much farther away from the valve plate during the suction process than in the discharge process. Hence, during the suction process the gas reaches the piston surface with lower velocity and higher temperature, explaining the smaller heat transfer in comparison with the cylinder and valve plate along period D in Figure 4.

It is interesting to note oscillations in the heat flux and mass flow rate during the discharge process (Figures 3 and 4), which are a result of the flow pattern in the valve. The mass flow rate through the valves can expressed as a function of both the effective flow area A_{ee} and the pressure difference between the cylinder and the discharge/suction chamber (Soedel, 2007):

$$\dot{m} = (A_{ee}/A_o)\dot{m}_{th} \tag{1}$$

where $\dot{m}$ and $\dot{m}_{th}$ represent the actual and theoretical mass flow rates through the valve, respectively, and A_o is the actual area of the valve orifice.

The effective flow area is affected by recirculating flow regions that periodically arise and disappear in the valve passage during the discharge process, as illustrated by numerical results for four crank angle positions (I, II, III and IV) in Figure 5. For instance, the presence of a recirculating flow region at position I reduces the area available for the flow and, as a consequence, it follows a decrease of mass flow rate and heat transfer in the cylinder. The mass flow rate and heat transfer decays then until the recirculating region disappears around ωt = 160° (position II). Although somewhat smaller, another recirculating flow region appears on the seat at the crank angle ωt = 163° (position III), restricting again the flow. As before, the mass flow rate decreases and the region of recirculation eventually is dissipated at position IV. Based on such observations, it can be concluded that intermittent recirculating flow regions in the valve passage is the phenomenon behind the oscillations of flow rate and heat transfer, as indicated in Figures 4 and 5. This mechanism is not observed in the suction process since the recirculating flow region in the suction valve is stable and remains on the seat until the valve closes.

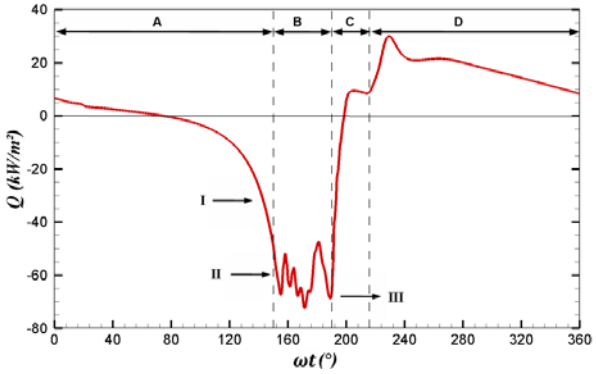

Figure 3: Predictions of heat flux in the cylinder.

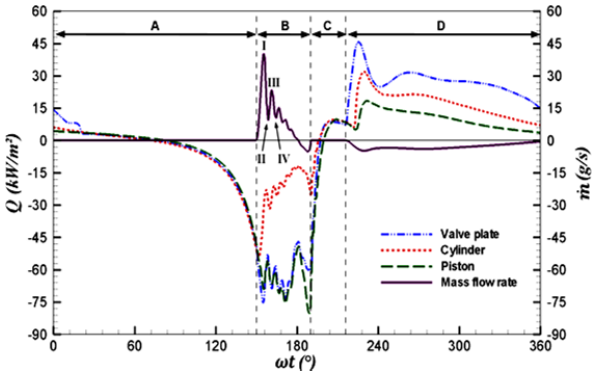

Figure 4: Heat fluxes at different surfaces in the compression camber and mass flow rate.

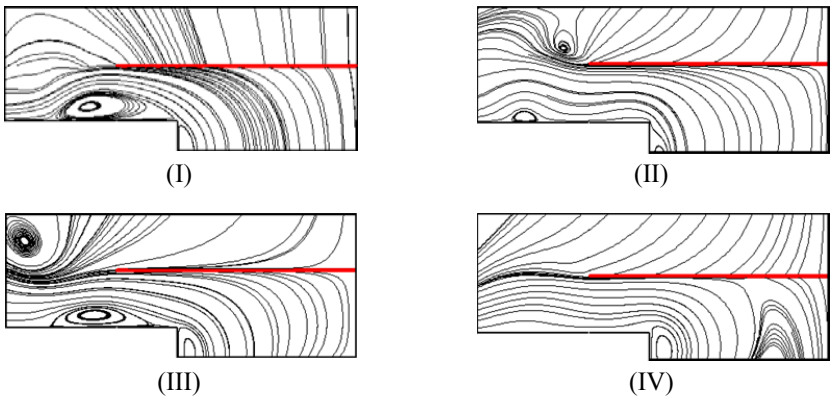

Figure 5: Periodic recirculating flow regions on the valve seat.

The present predictions of heat transfer inside the cylinder were compared to estimates returned by the correlations proposed by Adair *et al*. (1972) and Liu and Zhou (1984). In addition to that, the widely-known correlations developed for internal combustion engines by Annand (1963) and Woschni (1967) are also included in the comparisons. Annand (1963) determined a correlation for Nusselt number expressed as a function of a Reynolds number based on the piston mean velocity, whereas Woschni (1967) assumed a correlation for heat transfer with reference to the average velocity of the gas and instantaneous values of pressure and temperature in the cylinder.

Figures 6 shows a comparison between results of heat transfer, Q, predicted in this study and obtained with the aforementioned correlations. It is worth pointing out the great difference between the values of heat transfer returned by the different correlations. During the discharge process the correlations of Annand (1963) and Liu and Zhou (1984) indicate the highest levels of heat flux, whereas the proposals of Adair et al. (1972) and Woschni (1967) return the lowest estimates. The present model predicts intermediate values of Q in reasonable agreement with the correlation of Woschni (1967).

It should be noticed that an accurate account of the heat transfer during the suction process is particularly important for predicting gas superheating and, as consequence, volumetric and isentropic efficiencies. As one can see, all the correlations provide estimates of heat flux in the suction process much smaller than that predicted by the model developed in the present work. As far as the correlations of Annand (1963) and Whoschni (1967) are concerned, such a difference can be attributed to the different types of valves adopted in internal combustion engines and reciprocating compressors, which give rise to different flow patterns inside the cylinder, especially in the early stages of valve opening and closing, which directly affect the heat transfer process.

Mohammadi and Yaghoubi (2010) analysed different correlations for Nusselt and Reynolds numbers for an internal combustion engine operating at different speeds, by dividing the complete cycle into four processes: intake (I), compression (II), expansion (III), and exhaust (IV). With the use of numerical simulation, the authors obtained new heat transfer correlations for each one of such processes. Based on the same approach, we propose a new correlation for heat transfer inside the cylinder of reciprocating compressors, following Equation (2), but with different definitions for the Reynolds number and calibrated values for the constants *a*, *b* and *c*.

$$Nu = aRe^{b}Pr^{c} \tag{2}$$

where $Nu\ (= hD/K)$ and $Pr\ (= c_p\mu/K)$ are the Nusselt and Prandtl numbers. Moreover, D is the cylinder diameter, c_p is the specific heat at constant pressure and K is the thermal conductivity, respectively.

When the compression and expansion processes are considered and the valves are closed, the characteristic velocity for the Reynolds number is the piston mean velocity:

$$\overline{V_p} = 2Lf \tag{3}$$

where L is the piston stroke [m] and f is the compressor rotational speed [rad/s].

The main novelty of the correlation proposed herein is the definition of a characteristic velocity, V_c, for the Reynolds number during the suction and discharge processes, which is related to the mass flow rate $\dot{m}(t)$ through the valves:

$$V_c = \frac{|\dot{m}(t)|}{\rho(t)A_c} \tag{4}$$

where $\rho(\mathrm{t})$ is the gas density in the cylinder and $A_c\ (= \pi D^2/4)$ is the cross-sectional area of the cylinder.

In all processes, the characteristic length is represented by the diameter of the cylinder bore, *D*. The coefficient a and exponents b and c in Equation (2) were obtained from a curve fitting to the numerical results of heat transfer

inside the cylinder for a baseline operating condition, represented by ASHRAE LBP (T_e = -23.3ºC; T_c = 54.4ºC), refrigerant R-134a and rotational speed of 3000rpm. Due to the distinct phenomena taking place in the compression cycle, different definitions for the Reynolds number and different values for a, b and c were specified for the compression, discharge, expansion and suction processes, as indicated in Table 2.

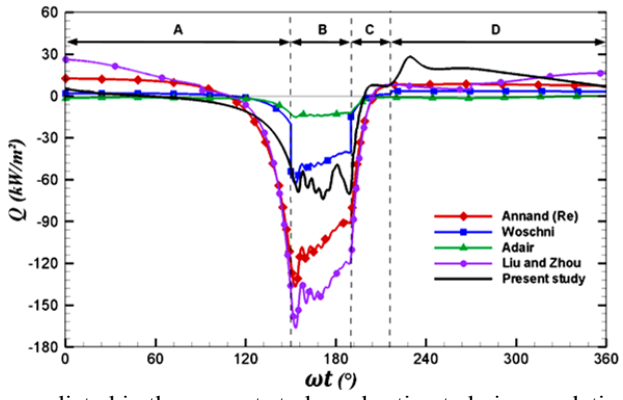

Figure 6: Heat fluxes predicted in the present study and estimated via correlations from the literature.

Table 2: Reynolds number and constants for each process of the compression cycle.

Process	Reynolds number	Constants
Compression	$Re = \frac{\rho(t) D \overline{V}_p}{\mu(t)}$	a = 0.08; b = 0.8; c = 0.6.
Discharge	$Re = \frac{\rho(t) D \left(\overline{V}_p + \overline{V}_p^{0.8} V_c(t)^{0.2}\right)}{\mu(t)}$	a = 0.08; b = 0.8; c = 0.6.
Expansion	$Re = \frac{\rho(t) D \overline{V}_p}{\mu(t)}$	a = 0.12; b = 0.8; c = 0.6.
Suction	$Re = \frac{\rho(t) D \left(\overline{V}_p + 2\overline{V}_p^{-0.4} V_c(t)^{1.4}\right)}{\mu(t)}$	a = 0.08; b = 0.9; c = 0.6.

In order to verify the generality of the new correlation, simulations were also carried out for different operating conditions, such as the compressor speed (1500rpm and 4500 rpm) and refrigerant fluid (R-600a) and pressure ratio, represented by the ASHRAE MBP (T_e = -6.7ºC; T_c = 54.4ºC) and HBP (T_e = 7.2ºC; T_c = 54.4ºC) conditions. As depicted in Figures 7, 8 and 9, the new correlation estimates the associated heat transfer in reasonable agreement with the numerical predictions in these quite different operating conditions.

Table 3 shows numerical predictions of heat transfer in the cylinder, $\dot{Q}$, in each process of the compression cycle for different operating conditions and the resulting net heat exchange between the gas and the cylinder. As can be seen, an increase in the evaporating temperature reduces the heat transfer $\dot{Q}$ in the compression, discharge and expansion processes, because the temperature of the gas becomes closer to the wall temperature. The fact that $\dot{Q}$ increases in the suction process is associated with two aspects: i) longer period of time in which the suction valve remains open and ii) higher velocity levels inside the cylinder associated with higher mass flow rate of the HBP condition. As expected, the increase of the compressor speed increases heat transfer. Finally, it is interesting to note that the greatest amount of heat is transferred to the gas during the suction process, making it evident the importance of predicting correctly this phenomenon given its importance on gas superheating. The net heat exchange is positive in all operating conditions, i.e., overall heat is released from the gas to the cylinder wall.

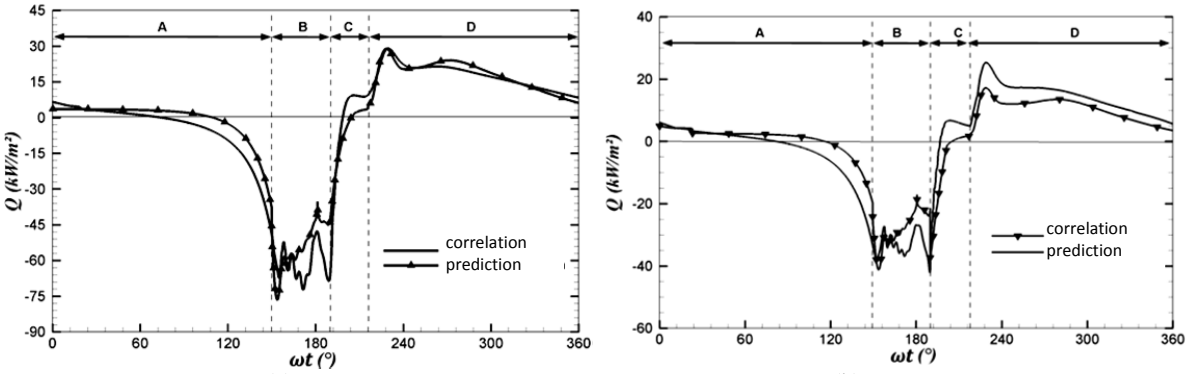

(a) R-134a. (b) R-600a.

Figure 7: Heat fluxes obtained numerically and with the new correlation for different refrigerants; compressor speed: 3000rpm; LBP condition: (T_e = -23.3ºC; T_c = 54.4ºC).

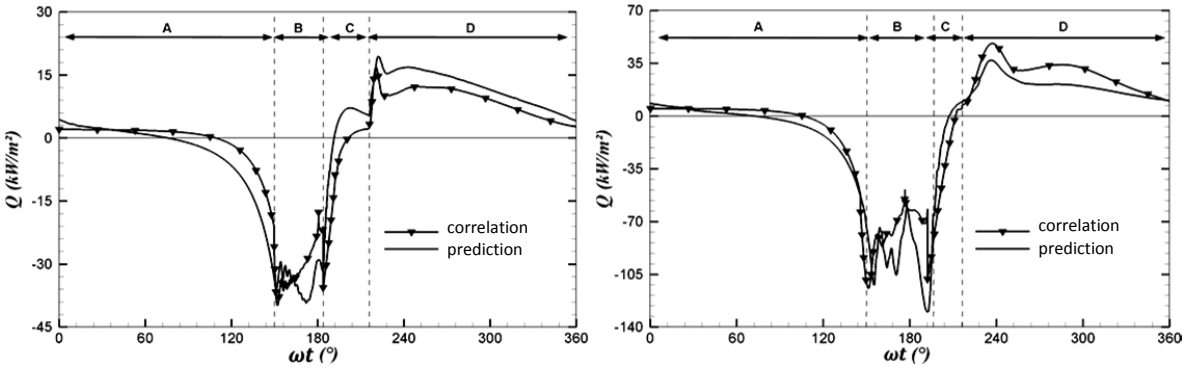

(a) 1500rpm. (b) 4500rpm.

Figure 8: Heat fluxes obtained numerically and with the new correlation for different compressor speeds; refrigerant: R-134a; LBP condition: (T_e = -23.3ºC; T_c = 54.4ºC).

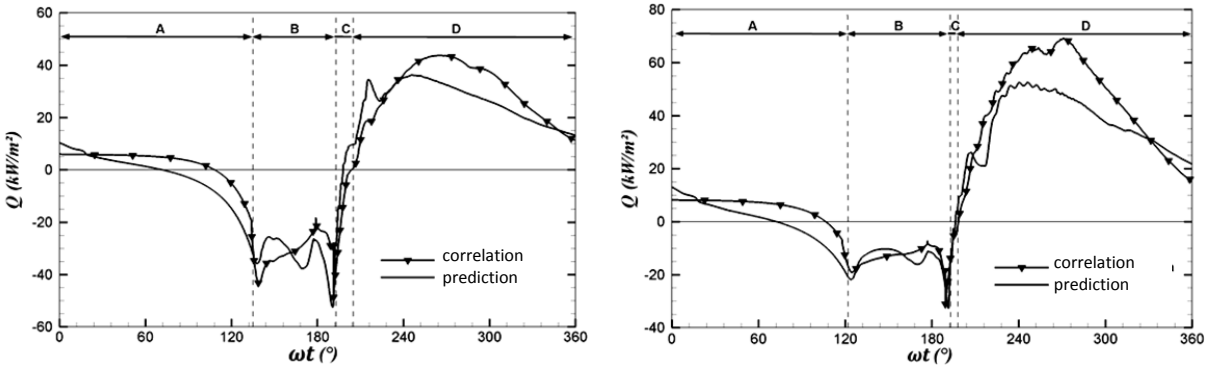

(a) MBP (T_e = -6.7ºC; T_c = 54.4ºC). (b) HBP (T_e = 7.2ºC; T_c = 54.4ºC).

Figure 9: Heat fluxes obtained numerically and with the new correlation for different pressure ratios; refrigerant: R-134a; compressor speed: 3000rpm.

Table 3: Heat transfer $\dot{Q}$ in the compression cycle for different operating conditions.

Operating conditions		$\dot{Q}$ [W]				
		Compression	Discharge	Expansion	Suction	Net
T_e (°C)	**-23.3**	-1.8	-4.2	-0.1	10.2	4.1
	-6.7	-1.4	-3.4	0.0	15.7	10.9
	7.2	-0.7	-2.0	0.0	22.2	19.5
Speed (rpm)	**1500**	-1.2	-2.1	0.1	6.9	3.7
	3000	-1.8	-4.2	-0.1	10.2	4.1
	4500	-2.6	-7.6	-0.4	11.6	1.0
Fluid	**R600a**	-1.1	-2.4	0.1	8.3	4.9
	R134a	-1.8	-4.2	-0.1	10.2	4.1

5. CONCLUSIONS

The present study considered the numerical modeling of the in-cylinder heat transfer of a small reciprocating compressor adopted for household refrigeration. The RNG k-ε turbulence model was used to predict the turbulent flow inside the cylinder, with a near wall modeling to resolve the viscous sublayer. The effect of both the suction and discharge processes on the heat transfer was also considered, with valve dynamics being described via a single degree-of-freedom model. It was shown that the in-cylinder flow induced during the suction and discharge processes gives rise to an increase of heat transfer inside the cylinder, not properly described by available heat transfer correlations. Based on the numerical results, a new proposal of heat transfer correlation for small reciprocating compressors was put forward and successfully applied to different operating conditions. In spite of that, further tests are still required to fully validate the proposed correlation.

NOMENCLATURE

D	Diameter of the cylinder bore	(m)	Q	Heat flux	(W/m^2)
k	Turbulent kinetic energy	(m^2/s^2)	Re	Reynolds number	-
L	Piston stroke	(m)	Re_y	Turbulent Reynolds number	-
$\dot{m}$	Mass flow rate	(kg/s)	T_c	Condensing temperature	(^{o}C)
Nu	Nusselt Number	-	T_e	Evaporating temperature	(^{o}C)
p_c	Condensing pressure	(kPa)	V_c	Piston mean speed	(m/s)
p_e	Evaporating pressure	(kPa)	y^+	Dimensionless distance to the wall	-
p	Pressure	(kPa)	μ	Dynamic viscosity	(Pa.s)
Pr	Prandtl number	-	ρ	Density	(kg/m^3)

REFERENCES

ANSYS Inc., 2010, ANSYS FLUENT *User Guide*.

Adair, R.P., Qvale, E.B., Pearson, J.T., 1972, Instantaneous Heat Transfer to the Cylinder Wall on Reciprocating Compressors, *Proc. Purdue Compressor Technology Conference*, West Lafayette, USA, pp. 521-526.

Annand, W.J.D., 1963, Heat Transfer in the Cylinders of Reciprocating Internal Combustion Engines, *Proc. Instn. Mech. Engnrs.*, vol. 117, pp. 973-996.

Brok, S.W., Touber, S., van der Meer, J.S., 1980, Modeling of Cylinder Heat Transfer - Large Effort, Little Effect?, *Proc. Purdue Compressor Technology Conference*, West Lafayette, USA, pp. 43-50.

Disconzi, F.P., Pereira, E.L.L., Deschamps, C.J., 2011, An Assessment of Modelling Approaches for Predicting Heat Transfer in the Cylinder of Small Reciprocating Compressors, *Proc. 23rd IIR International Congress of Refrigeration*, Prague, Czech Republic.

Fagotti, F., Todescat, M.L., Ferreira, R.T.S., Prata, A.T., 1994, Heat transfer modeling in a reciprocating compressor, *Proc. Purdue Compressor Technology Conference*, West Lafayette, USA, pp. 605-610.

Hsieh, W.H., Wu, T.T., 1996, Experimental Investigation of Heat Transfer in a High-Pressure Reciprocating Gas Compressor, *Experimental Thermal and Fluid Science*, vol. 13, p.44-54.

Kader, B., 1979, Temperature and Concentration Profiles in Fully Turbulent Boundary Layers, *Int. J. Heat Mass Transfer*, vol. 24, pp. 1541-1544.

Launder, B.E., Spalding, D.B., 1974, The Numerical Computation of Turbulent Flows, *Computer Methods in Applied Mechanics and Engineering*, vol. 3, pp. 269-289.

Launder, B.E., 1984, Numerical Computation of Convective Heat Transfer in Complex Turbulent Flows: Time to Abandon Wall Functions?, *Int. J. Heat and Mass Transfer*, Vol. 27, pp. 1485-1491.

Liu, R., Zhou, Z., 1984, Heat Transfer Between Gas and Cylinder Wall of Refrigeration Reciprocating Compressor, *Proc. Purdue Compressor Technology Conference*, West Lafayette, USA, pp. 110-115.

Mohammadi, A., Yaghoubi, M., Rashidi, M., 2008, Analysis of local convective heat transfer in a spark ignition engine, *International Communications in Heat and Mass Transfer*, vol. 35, pp. 215-224.

Mohammadi, A., Yaghoubi, M., 2010, Estimation of instantaneous local heat transfer coefficient in spark-ignition engines, *Int. J. Thermal Sciences*, vol. 49, pp. 1309-1317.

Overbye, V.D., Bennethum, J.E., Uyehara, O.A., Myers, P.S., 1961, Unsteady Heat Transfer in Engines, *SAE Transactions*, vol. 69, pp. 461-494.

Pereira, E.L.L., Deschamps, C.J., Ribas Jr, F.A., 2010, Numerical Analysis of Heat Transfer inside the Cylinder of Reciprocating Compressors in the Presence of Suction and Discharge Processes, *Proc. International Compressor Engineering Conference at Purdue*, West Lafayette, USA.

Rakopoulos, C.D., Mavropoulos, G.C., 2000, Experimental instantaneous heat fluxes in the cylinder head and exhaust manifold of an air-cooled diesel engine, *Energy Conversion & Management*, vol. 41, pp. 1265-1281.

Rakopoulos, C.D., Kosmadakis, G.M., Pariotis, E.G., 2010, Critical Evaluation of Current Heat Transfer Models Used in CFD In-Cylinder Engine Simulations and Establishment of a Comprehensive Wall-Function Formulation, *International Journal Applied Energy*, vol. 87, pp. 1612-1630.

Salinas-Casanova, D.A., Deschamps, C.J., Prata, A.T., 1999, Turbulent Flow through a Valve with Inclined Reeds, *Proc. Inter. Conf. on Compressors and Their Systems*, London, pp. 443-452.

Soedel, W., 2007, *Sound and Vibration of Positive Displacement Compressors*, CRC Press.

Woschni, G., 1967, Universally Applicable Equation for the Instantaneous Heat Transfer Coefficient in the Internal Combustion Engine, *SAE Transactions*, vol. 76, SAE paper 670931.

ACKNOWLEDGEMENTS

The material presented herein has been developed under a joint technical-scientific program between the Federal University of Santa Catarina and EMBRACO, partially funded by CNPq (Brazilian Research Council) through Grant No. 573581/2008-8 (National Institute of Science and Technology in Refrigeration and Thermophysics).